*Environ. Sci. Technol.* **2005**, *39,* 593−601

# Reactivity and Transformation of Antibacterial *N*-Oxides in the Presence of Manganese Oxide

HUICHUN ZHANG AND CHING-HUA HUANG*

*School of Civil and Environmental Engineering, Georgia Institute of Technology, Atlanta, Georgia 30332*

Organic *N*-oxides are an important structural class in many pharmaceutical and industrial chemicals. Little is known about the potential transformation of organic *N*-oxides at the sediment−water interface. Veterinary antibacterial agents carbadox and olaquindox are examples of commonly used heterocyclic *N*-oxides. Investigation with various *N*-oxides including carbadox, olaquindox, quinoline *N*-oxide, and quindoxin revealed surprisingly high reactivity toward $MnO_2$ for all of the compounds except olaquindox. Desoxycarbadox and quinoxaline, two structurally related compounds that lack an *N*-oxide functional group, showed much lower or no reactivity toward $MnO_2$. Comparisons among the previous compounds indicate that *N*-oxide moiety is the primary reactive site to $MnO_2$, and substitution at the α-C adjacent to the *N*-oxide group is critical in determining the overall reactivity. Reactions of *N*-oxides with $MnO_2$ appeared to be oxidation, with generation of $Mn^{2+}$ parallel to degradation of the parent organics. Product characterization confirmed that quinoline *N*-oxide and quindoxin transformed into 2-hydroxyquinoline and quinoxaline 2,3-diol, respectively, in reactions with $MnO_2$. The transformation involves separate steps of *N*-oxide moiety deoxygenation and neighboring α-C hydroxylation as elucidated by $^{18}O$ isotope experiments. All of the experimental results pointed to a mechanism that involves an *N*-oxide radical intermediate. This is the first study to report such transformation reactivity of organic *N*-oxides toward manganese oxide, offering a new degradation pathway that could be important for the fate of this group of compounds in the aquatic environment.

## Introduction

Quinoline *N*-oxides and quinoxaline *N,N*′-dioxides (example structures shown in Figure 1) represent organic *N*-oxides that are common in many pharmaceuticals, agrochemicals, and industrial chemicals (*1*, *2*). The *N*-oxide structure has also been observed in metabolites of many drugs and xenobiotics, as well as in intermediates of synthetic chemical processes because N atoms can undergo hydroxylation or oxidation to form *N*-oxides (*3*). Several quinoxaline *N,N*′-dioxides have been developed as potent antibacterial agents to promote growth and prevent dysentery and bacterial enteritis in farm animals (*4*−*6*). Among those, carbadox (methyl-3-(2-quinoxalinylmethylene)carbazate *N,N*′-dioxide) and olaquindox (2-methyl-3-[*N*-(2-hydroxyethyl)carbamoyl]-quinoxaline *N,N*′-dioxide) (Figure 1) have been widely used. It was found that carbadox and desoxycarbadox (Figure 1), a major metabolite of carbadox, are suspected carcinogens and mutagens (*4*, *5*). For this reason, carbadox has been banned in animal feed in Europe (*7*).

The common use of many organic *N*-oxides in various applications and their potential toxicities to humans and animals necessitate a better understanding of the environmental fate of these compounds to properly evaluate their risks. A comprehensive literature search revealed extremely limited information regarding abiotic or biotic transformation of *N*-oxides under environmental conditions. In particular, research on the potential transformation of *N*-oxides with metal oxides in soils is essentially nonexistent. So far, most of the published studies focused on the photolytic reactions of organic *N*-oxides. For example, photolytic activity of carbadox and desoxycarbadox has been observed during the process of sample preparation (i.e., fresh tissue samples were spiked with these compounds followed by extraction and cleanup with the whole process taking about 2 h (*8*)). The study showed that minimal incandescent light in the hood reached the samples and caused degradation especially for desoxycarbadox. Relatively extensive information has been published on the photochemical reactions of heterocyclic *N*-oxides in water or organic solvent media (reviewed in refs *2* and *9*). Thus, photolysis of organic *N*-oxides can be expected in most sun-lit environments. Mild sorption of olaquindox to various soil types with distribution coefficients $K_d$ in the range of 0.7−1.7 mL/g was documented (*10*). One study reported the possible aerobic and anaerobic biodegradation of olaquindox (50−5000 μg/L), with a slower degradation rate under anaerobic conditions (*11*).

In a recent occurrence study, no carbadox was detected in 104 samples from various locations in the United States at the method detection limit of 0.1 μg/L (*12*). Despite that, veterinary *N*-oxides such as carbadox and its metabolites may enter soils via manure applications or from feed wastes, while industrial *N*-oxides may enter aquatic systems from wastewater treatment plants. These *N*-oxides will likely end up in surface or groundwaters and have contact with soils and sediments. Manganese oxides are among the most important naturally occurring oxidants in facilitating organic pollutant transformation in soils and sediments and deserve particular attention due to their high reduction potentials. Previous work has demonstrated manganese oxides to be effective oxidants for a wide range of pollutants including substituted phenols (e.g., refs *13* and *14*) and anilines (e.g., refs *15* and *16*). A recent work by Li et al. (*17*) showed that soil Mn (III/IV) oxides play the most significant role, in addition to other soil components such as organic matter and iron oxides, in the irreversible oxidation and transformation of aromatic amines. As will be discussed later, this study demonstrates that certain organic *N*-oxides are highly susceptible to manganese oxide-facilitated oxidation.

In this study, veterinary antibacterials carbadox (CDX), olaquindox (ODX), and desoxycarbadox (desoxy-CDX) were investigated along with model compounds quinoline *N*-oxide (QNO), quinoxaline *N*-oxide (QXO), quindoxin (or quinoxaline *N,N*′-dioxide) (QDX), and quinoxaline (QX) (Figure 1) for reactions with Mn dioxide. A redox reaction pathway that has never been reported before for heterocyclic *N*-oxides and manganese oxide was discovered. On the basis of the results of kinetics, product characterization, and structurally related compound comparisons, schemes of this new reaction pathway were proposed.

* Corresponding author phone: (404)894-7694; fax: (404)894-8266; e-mail: ching-hua.huang@ce.gatech.edu.

10.1021/es048753z CCC: $30.25 
Published on Web 12/13/2004

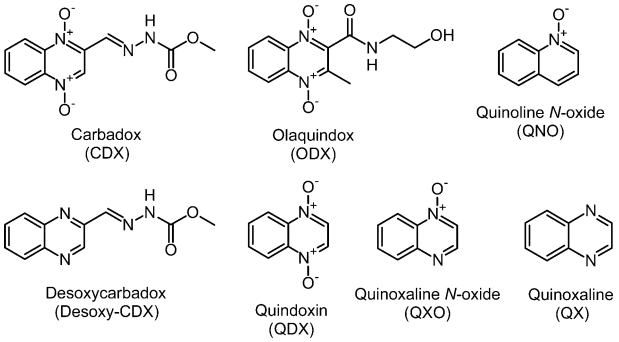


**FIGURE 1. Structures of organic *N*-oxides and related compounds investigated in this study.**

## Materials and Methods

**Chemical Reagents and Preparation.** Reagent-grade water (18.3 MΩ-cm resistivity) was prepared by a Millipore water purification system. CDX was purchased from Sigma (St. Louis, MO). ODX was obtained from ICN Biomedicals. QNO, QX, 2-hydroxyquinoline, 4-hydroxyquinoline, quinoxaline 2,3-diol, and methyltrioxorhenium were purchased from Aldrich. All the previous chemicals were at greater than 97% purity. $H_2{}^{18}O$ was obtained from Cambridge Isotope at 95% purity. Other employed chemical reagents were obtained from Fisher Scientific or Aldrich at greater than 98% purity (for solids) or of HPLC and GC grade (for solvents). All chemical reagents were used directly without further purification. Mn dioxide ($\delta$-$MnO_2$, similar to the naturally occurring birnessite) was synthesized based on the method by Murray (*18*) as reported by Zhang and Huang (*14*).

QDX was synthesized following the method from Coperet et al. (*19*). Briefly, QX (1.302 g) and methyltrioxorhenium (MTO 25 mg) were first mixed in 4 mL of methylene chloride ($MeCl_2$), followed by addition of 4 mL of 30% aqueous $H_2O_2$ solution (40 mmol). The resulting biphasic reaction mixture was continuously stirred for 16−20 h at 24 °C before being treated with a catalytic amount (2.5 mg) of $MnO_2$ and stirred for another hour until oxygen evolution ceased. Then, the reaction mixture was allowed to undergo phase separation. Afterward, the water layer was twice extracted with 4 mL of $MeCl_2$. The combined organic layers were dried over $Na_2SO_4$, filtered through glass fiber filters (47 mm, Pall Corporation), and concentrated under a gentle stream of nitrogen gas to give predominantly QDX and a trace amount of QXO. The mixture was then dissolved in approximately 2 mL of methanol and subjected to HPLC fraction collection. The collected QDX and QXO fractions were evaporated to dryness using a rotary evaporator, respectively. The purified QDX and QXO were kept in the freezer for storage. Coperet et al. (*19*) reported a yield of 98% for QDX. The yields of QDX and QXO in this study were not determined.

Desoxy-CDX was synthesized following the method by Massy and McKillop (*20*). Briefly, CDX (6.0 g) was dispersed in 120 mL of acetic acid and the mixture was refluxed briefly and then cooled rapidly to 26 °C. $Na_2S_2O_4$ (85%, 10.56 g) was dissolved in 60 mL of cold water, and the solution was immediately added to the stirred dispersion, accompanied by a temperature rise to 33 °C. After being stirred for 1 h, the mixture was placed in a rotary evaporator to evaporate to dryness. After the sample was dried, 60 mL of water was added to the residue, and the resulting mixture was cooled to 4 °C in a refrigerator overnight. The mixture was filtered through glass fiber filters, and the collected solids were washed three times with 6 mL of water. After vacuum drying, brown crystalline desoxy-CDX was obtained. Massy and McKillop (*20*) reported a 66% yield of desoxy-CDX. Although the yield in this study was not determined, the synthesized desoxy-CDX appeared to be satisfactorily pure based on high peak purity observed by HPLC with a diode-array UV/vis detector.

Stocks of *N*-oxides and related model compounds were prepared in pure methanol at 100−120 mg/L. All stocks were stored at 4 °C and used within a month of preparation.

**Reactor Setup.** The experimental setup for the reaction of *N*-oxides with $MnO_2$ is similar to that used in the previous study (*14*). Briefly, all experiments were conducted in 25 mL screw-cap amber glass bottles with Teflon septa, under constant stirring in a 22 °C water basin. Reaction pH was maintained with 10 mM acetate (pH 4−5), 4-morpholinepropanesulfonic acid (MOPS) (pH 6−8), or 2-(cyclohexylamino)ethanesulfonic acid (CHES) (pH 9−10) buffers. Reactions were initiated by adding a certain amount of organic stock to solutions containing manganese oxide, buffer, and constant ionic medium. Aliquots were periodically collected, and reactions were quenched immediately for analyses either by centrifugation (at 12 000 rev/min for 20 min) or by ascorbic acid (0.1 M) addition. Typical reaction times were from hours to several days. Controls with *N*-oxides alone and with reaction media alone were prepared simultaneously with each batch of reaction.

**Analysis of *N*-Oxides and $Mn^{II}$ Ions.** Decrease in the concentrations of *N*-oxides and other structurally related compounds was monitored by a reverse-phase high performance liquid chromatography (HPLC) system with a Zorbax RX-C18 column (4.6 × 250 mm, 5 $\mu$m) and a diode-array UV/vis detector (DAD) (1100, Agilent Technology). CDX and desoxy-CDX were detected at 308 nm, and ODX was detected at 262 nm by the UV detector. All the other compounds were detected at 230 nm. The mobile phase consisted of a solution containing 20 mM ammonia acetate (eluent A) and acetonitrile (eluent B) at a flow rate of 1 mL/min. The mobile phase began with 5% B (95% A), increased to 60% B in 10 min, and increased to 95% B until 11 min, and then the column was flushed thoroughly under these conditions for 4 min followed by a 4 min post time that allowed reequilibration of the column.

Generation of $Mn^{II}$ ions from reductive dissolution of Mn dioxide was monitored using an inductively coupled plasma (ICP) spectrometer (Thermo Jarrell Ash Trace Analyzer) (for details of the analytical procedure, see ref *14*). Controls with only manganese oxide, electrolytes, and pH buffers revealed that dissolution of Mn dioxide did not occur in the absence of the *N*-oxides.

**Analysis of Organic Products.** Reaction products were analyzed by a HPLC/DAD/MS system with a Zorbax SB-C18 column (2.4 × 150 mm, 5 $\mu$m) (1100/1100MSD, Agilent Technology). Typically, 20 mL of reaction suspensions containing 0.1 mM of *N*-oxides and 1 mM $MnO_2$ was prepared at pH 4 to generate a sufficient amount of products for LC/MS analysis. Reaction products were the same at the other pH values investigated in this study. Product analyses were also conducted in reaction suspensions prepared in $H_2{}^{18}O$, and the pH was adjusted by adding a small amount of 0.1 M HCl with the other conditions the same as those in the regular water. The $H_2{}^{18}O$ reaction suspensions were equilibrated overnight before adding the *N*-oxide stock to initiate the reaction. Reactions were quenched after 1−7 days by centrifugation (at 12 000 rev/min for 20 min), and the supernatants were analyzed by LC/MS. Gradient elution was conducted using pure acetonitrile and 0.02% acetic acid in 90:10 water/acetonitrile (v/v) at a flow rate of 0.20 mL/min. The MS analysis was conducted by electrospray positive ionization at the fragmentation voltage 80−120 V with mass scan range 50−1000 $m/z$. Other LC/MS instrumental parameters were similar to those reported previously (*14*).

**TABLE 1. Kinetic Comparison among Organic *N*-Oxides and Related Compounds[a]**

| compound | $r_{init}$ ($\mu$M h$^{-1}$)[b] | adsorption (%)[c] |
|---|---|---|
| quindoxin (QDX) | 6.9 ± 0.6 | <10 |
| quinoxaline *N*-oxide (QXO) | 3.8 ± 0.2 | <14 |
| quinoline *N*-oxide (QNO) | 3.1 ± 0.1 | ~0 |
| carbadox (CDX) | 3.0 ± 0.2 | <10 |
| desoxycarbadox (desoxy-CDX) | 3.5 ± 0.8 × 10$^{-2}$ | not determined |
| olaquindox (ODX) | no reaction | ~0 |
| quinoxaline (QX) | no reaction | ~0 |

[a] Typical reaction conditions: 1 mM $MnO_2$, 10 $\mu$M organic compound, 0.01 M pH 4 buffer, 0.01 M NaCl, 22 °C. [b] The initial reaction rates are reported with 95% confidence levels from replicates of experiments. [c] Adsorption % = $C_{ads}/C_{total}$ in %.

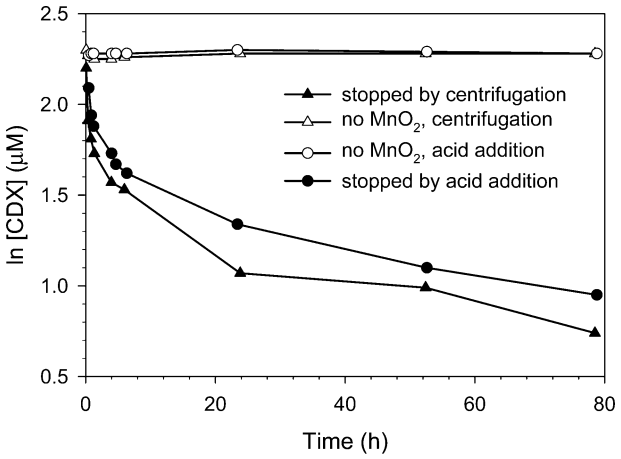


**FIGURE 2. Time course of CDX oxidation by $MnO_2$. Reactions contained 1 mM $MnO_2$ and 10 $\mu$M CDX initially with pH 4 acetate buffer at 22 °C.**

## Results and Discussion

**Reaction Kinetics.** In the absence of manganese oxide, all of the *N*-oxides investigated in this study were stable under the experimental conditions, and no measurable loss of the compounds could be detected after a week. In contrast, significant degradation of *N*-oxides (CDX, QDX, QXO, and QNO) occurred in the presence of $MnO_2$ (Table 1). A typical time course of CDX reaction with $MnO_2$ is shown in the ln-[CDX] versus time semilog plot (Figure 2). The data showed that the reaction kinetics deviated from the pseudo-first-order kinetics even over the first few time increments. Similar kinetic behavior was observed for all the other *N*-oxides. For the sake of comparison, reaction kinetics were evaluated based upon initial reaction rate $r_{init}$ (= $-dC/dt$) in $\mu$M h$^{-1}$ (i.e., the slopes over the first few time increments in plotting concentration vs time (at reaction time of ~2 h, with $R^2 \geq 0.95$ for the linearization)). Such complicated kinetic behavior involving manganese oxide surfaces has also been observed in many previous studies (e.g., refs *13*−*15*).

The data in Table 1 showed that QDX reacted at the fastest rate with $MnO_2$. QXO, QNO, and CDX reacted at similar initial reaction rates that were approximately half of the rate of QDX. Desoxy-CDX reacted 2 orders of magnitude slower than CDX. ODX appeared to behave differently from the previous *N*-oxides, with no detectable degradation for up to a week. The structurally related but non-*N*-oxide quinoxaline also did not react with $MnO_2$.

A series of experiments with varying CDX loadings (5−50 $\mu$M) but a fixed $MnO_2$ loading (1 or 3 mM) or with varying manganese oxide loadings (0.1−3 mM) but a fixed CDX loading (10 $\mu$M) were conducted to assess the initial reaction orders with respect to CDX and $MnO_2$ (Figure 3a). When CDX loading was below 20 $\mu$M, the log of the initial reaction rate $r_{init}$ increased linearly with the log of CDX loading with slopes of 0.55−0.58. However, when CDX loading was above 20 $\mu$M, log $r_{init}$ appeared to fall below the linear increase, suggesting that surface saturation might be approached in the presence of higher concentration of CDX. This phenomenon is similar to the observations in the previous work (*14*), in which an increase in the reaction rate of the phenolic antiseptic triclosan with a fixed amount of $MnO_2$ (in molar excess to triclosan) quickly tapered off with increasing triclosan concentration. This present study also demonstrates that $MnO_2$, even at over 20-fold molar excess, can be saturated by a small amount of CDX molecules, suggesting that the number of reactive surfaces sites is rather limited. For $MnO_2$, a slope of 0.54 was obtained by plotting log $r_{init}$ versus the log of $MnO_2$ loading across the range investigated. These results demonstrated that the reaction order with respect to either CDX or $MnO_2$ was constant and quite comparable within a suitable concentration range of either reactant. To minimize further complication of the surface kinetics, subsequent studies were conducted within the concentration range where the constant reaction order of either reactant had been determined.

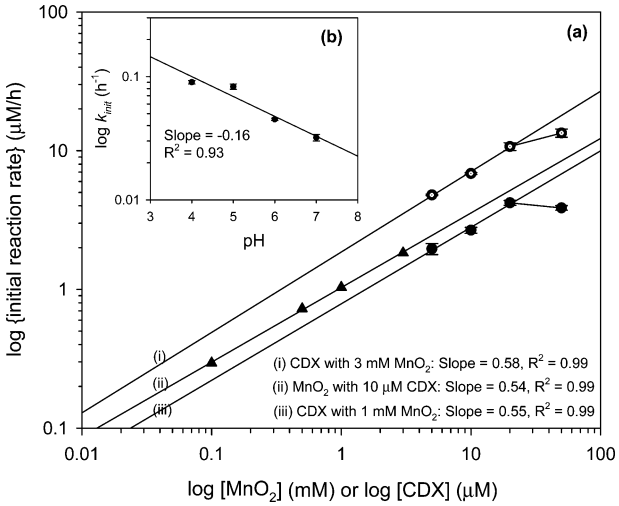


**FIGURE 3. Reaction orders with respect to (a) CDX and $MnO_2$ at pH 4 and 22 °C and (b) pH, with 10 $\mu$M CDX and 3 mM $MnO_2$ initially at 22 °C. The data are reported with 95% confidence levels when applicable.**

The initial reaction rate constant $k_{init}$ in $\mu M_{CDX}^{-0.56}$ h$^{-1}$ (i.e., the initial reaction rate divided by the initial CDX concentration to the power of 0.56, $r_{init} = -dC/dt = -k_{init}[CDX]^{0.56}$) was also estimated to evaluate the reaction order with respect to [H$^+$] ($k_{init} = k_{pH}[H^+]^a$). Solution pH apparently affected the reaction rate of CDX with manganese oxide significantly, with log $k_{init}$ decreasing linearly with increasing pH (CDX degradation rate at pH > 7 was too slow to be observed within 2 weeks). Least-squares fitting of Figure 3b data gives an average reaction order of 0.16 for H$^+$. Adsorption of CDX to manganese oxide surfaces under different pH values was evaluated by comparing the measured CDX concentrations from two different reaction quenching methods (i.e., ascorbic acid addition vs centrifugation) as described in the previous study (*14*). By adding ascorbic acid, manganese oxide was rapidly reductively dissolved yielding $Mn^{2+}$ ions; thus, the adsorbed yet unreacted CDX on the oxide surface could be released and measured (control experiments have verified the stability of CDX in the presence of ascorbic acid). In contrast, only the nonadsorbed CDX could be detected in the centrifugation supernatant. This comparison showed that less than 10% of CDX was adsorbed to $MnO_2$ at pH 4 (Table 1) to 9. Low adsorption extent (<14%) to $MnO_2$ was also seen with the other *N*-oxides by the same approach (Table 1).

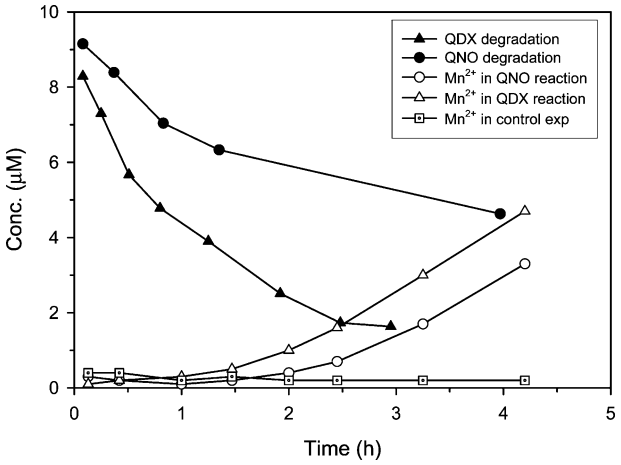


**FIGURE 4. Time course of QDX or QNO degradation and corresponding $Mn^{2+}$ generation. Reaction conditions are the same as Table 1.**

On the basis of the previous kinetic results, the initial reaction rate of CDX with $MnO_2$ can be described by the following kinetic expression:

$$\text{initial rate } (r_{\text{init}}) = -\frac{\text{d[CDX]}}{\text{d}t} = -k_{\text{init}}[\text{CDX}]^{0.56} = -k_{\text{exp}}[\text{CDX}]^{0.56}[\text{MnO}_2]^{0.54}[\text{H}^+]^{0.16} \quad (1)$$

From the values of $r_{\text{init}}$ at various $MnO_2$ loadings and pH values, the third-order rate constant $k_{\text{exp}}$ (applicable within the employed experimental conditions) was computed to be $2.98 \pm 0.48 \times 10^5\ M_{CDX}^{0.44}\ M_{MnO_2}^{-0.54}\ M_{H^+}^{-0.16}\ h^{-1}$ ($n = 30$) for CDX.

Production of $Mn^{2+}$ ions from reductive dissolution of $MnO_2$ by QDX or QNO was monitored, and a continuous increase in $Mn^{2+}$ concentration was observed as degradation of the *N*-oxides proceeded (Figure 4). It was, however, difficult to determine the exact concentration of $Mn^{2+}$ generated, particularly at the initial stage of the reaction, due to strong adsorption of $Mn^{2+}$ to $MnO_2$. Experiments showed that greater than 90% of 10 $\mu$M $Mn^{2+}$ was adsorbed to 1 mM $MnO_2$ at various pH values ($4 < pH < 7$). Nevertheless, the increase in $Mn^{2+}$ corresponding to the loss of either QDX or QNO provided the evidence that manganese oxide was reductively dissolved by *N*-oxides yielding $Mn^{2+}$. The data in Figure 4 (particularly after 2 h of reaction time) also showed that a greater amount of $Mn^{2+}$ was generated in reaction of QDX (with two *N*-oxide groups) than that of QNO (with one *N*-oxide group) at any reaction time.

**Oxidation Products of QNO and QDX.** Electrospray LC/MS analyses of QNO ($m/z$ 146) reaction mixtures exhibited the existence of one major product ($m/z$ 146) and one minor product ($m/z$ 305) (Figure 5a). The parent QNO and its major reaction product had the same molecular weight but exhibited different fragmentation patterns. The parent QNO fragmented by the loss of OH from the *N*-oxide position (i.e., $-m/z$ 17) (Figure 5b), consistent with the previous work by Miao et al. (*21*) in which detailed fragmentation pathways of QNO were documented. In contrast, the major product of QNO fragmented by the loss of $H_2O$ (i.e., $-m/z$ 18), a fragmentation pattern often involves a hydroxyl substituent on the compound (Figure 5c). Authentic standards of 2-hydroxyquinoline and 4-hydroxyquinoline were analyzed by electrospray LC/MS under the same conditions. 2-Hydroxyquinoline and 4-hydroxyquinoline exhibited the same mass spectrum but had different retention times. The LC retention time and MS spectrum of 2-hydroxyquinoline matched with those of the major product of QNO, confirming the major product to be 2-hydroxyquinoline. For the minor product, the molecular ion of 305 was assigned based on the difference of 22 in $m/z$ 327 ($[M + Na]^+$) and $m/z$ 305 ($[M + H]^+$). There were two fragments, $m/z$ 146 and 160, in the minor product, suggesting that the product could be an adduct of QNO or 2-hydroxyquinoline with a reaction intermediate (see Table S1a in the Supporting Information for spectral information).

Analyses of the oxidation products of QNO (at pH 4) over the period of 39 h (Figure 6a) showed that the MS peak area of the $m/z$ 305 product increased slightly in the beginning and then quickly decreased until disappearance. This kinetic behavior indicates that the $m/z$ 305 product is a reaction intermediate. The product evolution study showed that the abundance of 2-hydroxylquinoline consistently increased over time, suggesting it being a stable end product. Separate experiments with 2-hydroxyquinoline also confirmed that this compound is stable in the presence of manganese oxide. Moreover, at any reaction time, the sum of QNO and 2-hydroxylquinoline accounted for more than 95% of the initial QNO, indicating that 2-hydroxylquinoline is the dominant product.

LC/MS analyses of QDX ($m/z$ 163) reaction mixtures indicated the presence of primarily two products: $m/z$ 163

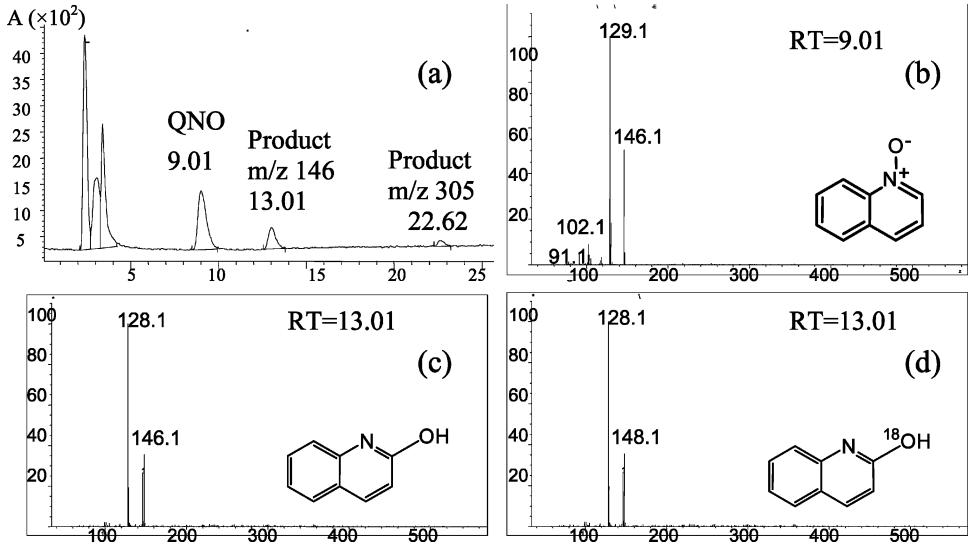


**FIGURE 5. LC/MS analyses of QNO and reaction products: (a) LC/MS chromatogram, (b) spectrum of QNO, (c) spectrum of 2-hydroxyquinoline product, and (d) spectrum of 2-hydroxyquinoline ($^{18}O$) product in $H_2{}^{18}O$ reaction medium.**

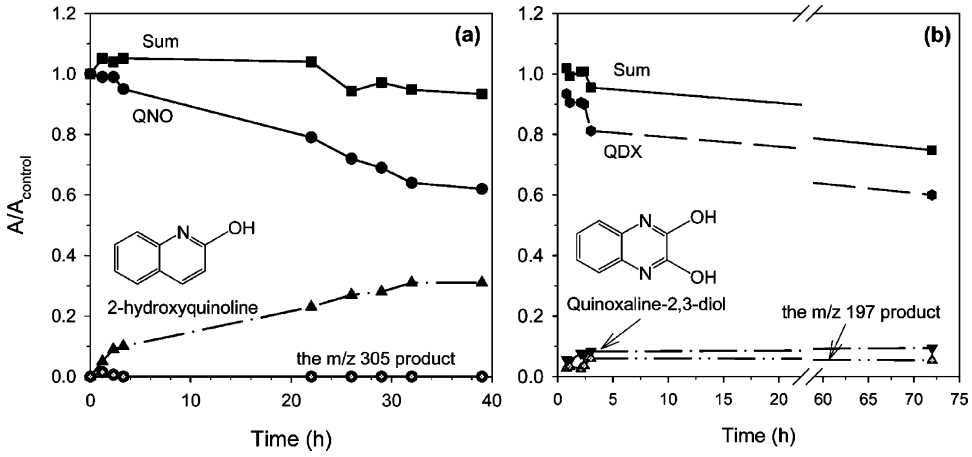


**FIGURE 6. Product evolution for the reaction of (a) QNO and (b) QDX with $MnO_2$ ($A$ = LC/MS peak area; $A_{control}$ = LC/MS peak area of QNO or QDX in the oxide-free control experiments; sum was calculated based on the total area of parent compound and products).**

(major) and 197 (minor). The molecular ions of these two products were assigned based on the observation of the sodiated ions $[M + Na]^+$ and the molecular ions $[M + H]^+$ (Supporting Information Table S1c). Similar to the case of QNO, QDX and its major product had the same molecular weight but different fragmentation patterns. QDX exhibited the characteristic loss of OH (i.e., $-m/z$ 17) from one of its *N*-oxide groups, while the $m/z$ 163 product yielded little fragmentation. The $m/z$ 163 product was confirmed to be quinoxaline 2,3-diol (structure shown in Figure 6b) by matching the LC retention time and MS spectrum with an authentic standard of this compound. The structure of the $m/z$ 197 minor product could not be determined based on its LC/MS spectra.

Product evolution study of QDX (Figure 6b) revealed that quinoxaline 2,3-diol and $m/z$ 197 products were stable end products. Quinoxaline 2,3-diol was present at abundance almost twice as much as the $m/z$ 197 product. The inertness of quinoxaline 2,3-diol toward manganese oxide under the reaction conditions was confirmed by kinetic experiments that lasted up to 5 days. As shown in Figure 6b, the sum of QDX, quinoxaline 2,3-diol, and the $m/z$ 197 products gradually decreased over time. For example, about 75% of mass balance was obtained at reaction time of 72 h, indicating that other unknown product(s) could also be present but were undetectable by the current approach. Thus, the oxidation of *N,N′*-dioxide QDX appeared to be more complex than the oxidation of *N*-monooxide QNO.

Information regarding chemical oxidation of *N*-oxides is rather limited. Published results on the photoreactions of *N*-oxides were reviewed to gain insights into the products observed in this study. Previous work proposed that photoreaction of QDX in water proceeded via an intermediate with a three-membered ring among O, N, and the neighboring α-C atoms on QDX, followed by rearrangement of the three-membered ring to form a 2-hydroxyl substituent on the product (reviewed in ref *9*). To discern whether the same type of rearrangement was the mechanism behind the formation of 2-hydroxyquinoline from QNO, isotope experiments in $H_2{}^{18}O$ were conducted to test this hypothesis. If the oxidation of QNO in $H_2{}^{18}O$ yielded the same $m/z$ 146 product, it would be evident that the O atom of the *N*-oxide rearranged to form the −OH substituent in 2-hydroxyquinoline. In fact, the oxidation of QNO by manganese oxide in $H_2{}^{18}O$ yielded one major product of $m/z$ 148 and one minor product of $m/z$ 309, with the same retention times as the previous $m/z$ 146 and 305 products, but 2 and 4 masses higher, respectively (Figure 5c and Table S1b). The $m/z$ 148 product had the same major fragment ($m/z$ 128) as 2-hydroxyquinoline, corresponding to the loss of $H_2{}^{18}O$ (−20) from $^{18}O$-labeled 2-hydroxyquinoline (Figure 5c). The $m/z$ 309 product had two major fragments: $m/z$ 148 and 162. Each of the fragments was 2 masses higher than the corresponding fragment in the $m/z$ 305 product, indicating the presence of one $^{18}O$ atom in each fragment (Table S1b). Thus, the isotope experiments confirm that rearrangement of the *N*-oxide group is not involved in the production of 2-hydroxyquinoline from QNO. Instead, the loss of the O atom from the *N*-oxide group and the formation of the 2-OH substituent are likely two separate steps. The source of the 2-OH substituent may be from the bulk water or −OH groups associated with the manganese oxide skeleton, which is discussed further in a later section. The results with the $m/z$ 309 product support that this minor product may be an adduct of 2-hydroxyquinoline (not QNO) with a reaction intermediate (as postulated in Scheme 1).

**Oxidation Products of CDX and Desoxy-CDX.** LC/MS analyses of CDX reaction mixtures indicated more complicated reaction products than the cases discussed previously (Table S1d). The molecular ion of CDX is $m/z$ 263, and its main fragment ($m/z$ 231) corresponds to the loss of $-OCH_3$ (i.e., $-m/z$ 32) from the side chain (detailed fragmentation pathways were proposed in ref *21*). Four products were detected by LC/MS and could be of molecular $m/z$ of 281, 279, 205, and 197, respectively (assigned based on the observation of $[M + Na]^+$ and $[M + H]^+$ ions). For the $m/z$ 279 product, the major fragment $m/z$ 263 corresponded to the loss of one O atom (i.e., $-m/z$ 16) from the molecular ion. Two other fragment ions $m/z$ 247 and 231 corresponded to the loss of $-OCH_3$ (i.e., $-m/z$ 32) from the molecular ion (i.e., $m/z$ 279) and from the main fragment $m/z$ 263, respectively. These results indicated that the $m/z$ 279 product could be a CDX analogue with an O atom addition (the postulated structure can be seen in Scheme 2). The other three products ($m/z$ 281, 205, and 197) had small MS responses, and the structure identification could not be achieved based on their spectra. In addition to the previous four products, UV detection (220 nm) of CDX reaction mixtures revealed the presence of two extra products without any MS responses, despite the fact that the following LC/MS conditions were also tried: (i) using formic acid instead of acetic acid in the mobile phase, (ii) changing to electrospray negative ionization mode, and (iii) applying either positive or negative atmospheric pressure chemical ionization (APCI) instead of electrospray ionization.

Monitoring the reaction products of CDX (at pH 4) over several hours further revealed that the $m/z$ 279 product was actually an intermediate, with its MS area increasing slightly in the beginning followed by a rapid disappearance (resembling the kinetic behavior of the $m/z$ 305 product in the oxidation of QNO by $MnO_2$, Figure 6a). All other products

**SCHEME 1. Proposed Reaction Pathway of QNO in the Presence of $MnO_2$**

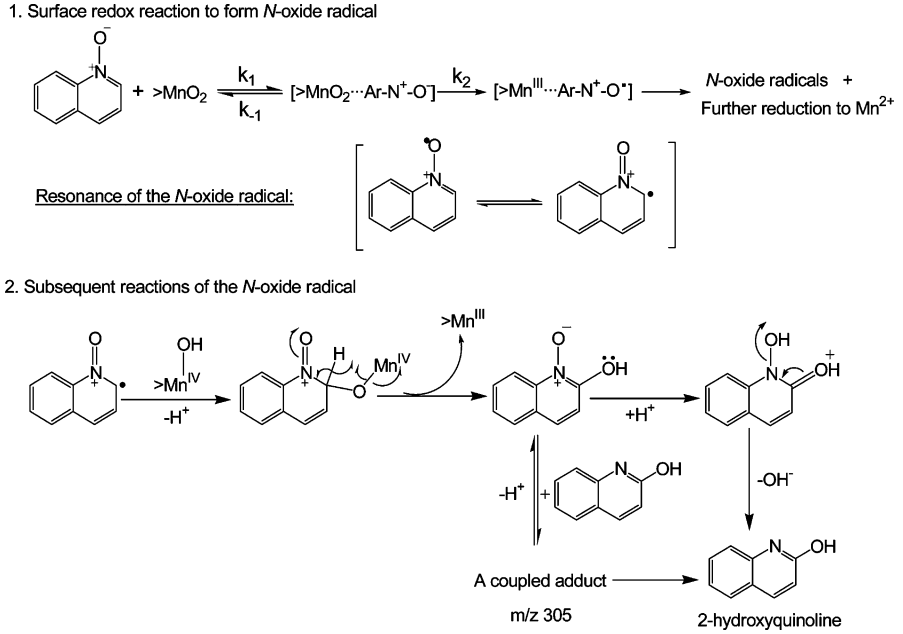


**SCHEME 2. Proposed Reaction Pathway of CDX in the Presence of $MnO_2$**

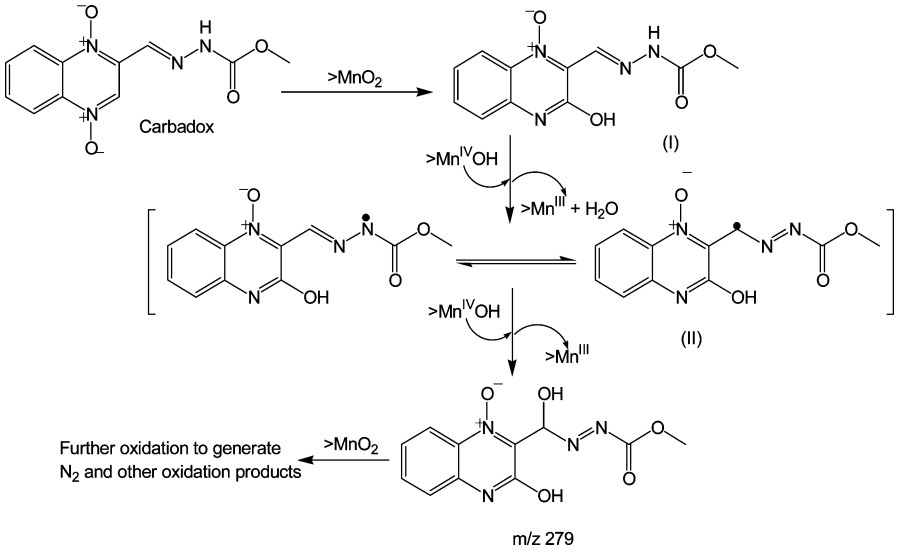


displayed their small MS/UV responses throughout the reaction period for up to 1 week.

The same fragmentation pattern as that of CDX was observed for desoxy-CDX, with the molecular ion $m/z$ 231 and the major fragment $m/z$ 199 (i.e., after loss of $-OCH_3$) (Table S1e). No appreciable products were detected in desoxy-CDX oxidation mixtures for up to 1 week because less than 10% of the parent compound was degraded under the employed experimental conditions.

**Chemical Reaction Sites and Reactivity.** The much higher reactivity of the *N*-oxide compounds (QDX, QNO, QXO, CDX) versus the non-*N*-oxide compounds (QX, desoxy-CDX) (Table 1 and Figure 1) indicates that the *N*-oxide functional group is a dominant reactive site in the oxidation with $MnO_2$. The average 2-fold higher reactivity of QDX (*N*,*N*′-dioxide) versus QNO and QXO (*N*-oxide) also supports the previous conclusion, with the presence of two versus one reactive *N*-oxide moieties, respectively. The slow reaction rate of desoxy-CDX versus the inactivity of QX indicates that the side chain of CDX and desoxy-CDX can also react with $MnO_2$ but with a much lower reactivity than the *N*-oxide moiety. This observation is consistent with the susceptibility of hydrazide (−CO−NH−N<) or hydrazone (> CH═N−N<) moieties toward oxidation reactions (*22*, *23*).

Both CDX and ODX contain two *N*-oxide functional groups; however, CDX has reactivity similar to *N*-oxide (rather than *N*,*N*′-dioxide), while ODX does not react with $MnO_2$ at all. Compared to QDX, CDX has one substituted side chain α-adjacent to one of its *N*-oxide groups, while ODX has one amide (−CO−NH−) side chain and one methyl substituent next to either of its *N*-oxide functional groups, respectively (Figure 1). The amide side chain of ODX is not expected to undergo redox reaction with $MnO_2$. As discussed in the preceding sections, characterization of the QNO and QDX oxidation products reveals that oxidation of the *N*-oxide group by $MnO_2$ requires hydroxylation at its neighboring α-C position. In other words, the reactivity of one of the *N*-oxide groups in CDX, and of both of the *N*-oxide groups in ODX, is retarded due to blockage at the α-C position by replacing the α-H by an alkyl substituent.

**Surface Reactions.** A general surface reaction mechanism involving manganese oxides has been extensively reported

(e.g., refs *13*−*15*). In summary, the organic compound in question is adsorbed to the oxide surface, forming a precursor complex. Electrons are transferred within the precursor complex, followed by the release of organic oxidation products and $Mn^{2+}$. The precursor complex formation and electron transfer are likely rate-limiting. Oxidation of *N*-oxides by $MnO_2$ is likely to follow this surface reaction mechanism as do many other organic contaminants. For example, the reaction kinetics of CDX observed in this study supports this conclusion as discussed next.

The initial reaction orders of CDX, $MnO_2$, and $H^+$ were determined to be 0.56, 0.54, and 0.16, respectively (Figure 3 and eq 1). The linear dependence of CDX oxidation rate on pH is mainly due to the linear dependence of the reduction potential of $MnO_2$ on pH. In other words, the oxidizing power of $MnO_2$ decreases with increase in pH, which leads to decreasing reaction rate (Figure 3b). Such a phenomenon was also seen in many previous studies (e.g., refs *13*−*15*).

Higher reaction orders with respect to reactants were found by the authors in a previous study, in which oxidation of two phenolic antibacterial agents, triclosan and chlorophene, by manganese oxides was examined (*14*). In that study, the reaction orders were about 1, 1, and 0.5 for triclosan, $MnO_2$, and $H^+$, respectively. A much higher adsorption of triclosan toward manganese oxide was also observed. For example, over 55% of triclosan (initial concentration of 10 $\mu$M) was adsorbed to 0.1 mM of $MnO_2$ at pH 5. In contrast, less than 10% of CDX (initial concentration of 10 $\mu$M) was adsorbed to 1 mM $MnO_2$ within the pH range of 4−9. The smaller reaction orders observed in the current study than those in the previous one could be related to the weak adsorption of the *N*-oxides to $MnO_2$. As illustrated in much of the earlier work, precursor complex formation and electron transfer are likely rate-limiting (e.g., refs *13* and*14*), and the overall dependence of the reaction rate on each of the reactants (i.e., the reaction order of each reactant) would be influenced by the reaction rates of these two steps. Adsorption of the organic reductant to $MnO_2$ has a significant impact on the overall surface oxidation rate through affecting the precursor complex formation (e.g., refs *13* and *14*). Weaker adsorption would lead to poorer precursor complex formation, a slower reaction rate, and thus less sensitivity of the reaction rate to the change in the reactant concentration. Such an effect would be reflected as smaller reaction orders for the reactants in the first elementary reaction (i.e., precursor complex formation) and hence in the overall reaction rate. A similar phenomenon was also observed in the oxidation of fluoroquinolone antibacterial agents and related amine compounds by goethite (α-FeOOH) (*24*). In this particular study by the authors, 1-phenylpiperazine had a smaller reaction order (0.54) than ciprofloxacin (0.67−0.71), possibly due to the much stronger adsorption of ciprofloxacin to goethite than that of 1-phenylpiperazine.

The same reaction orders of CDX and $MnO_2$ indicates that these two reactants are consumed at an equal rate, with an average of two electrons transferred from CDX to $MnO_2$ to generate $Mn^{2+}$ ions. The fact that the rate of corresponding $Mn^{2+}$ generation is comparable to that of QDX degradation (Figure 4) is also consistent with the observed reaction orders and supports the previous conclusion.

**Reaction Schemes.** Studies have shown that deoxygenation of QDX in the presence of nucleophiles such as $S_2O_4^-$ or $AcO^-$ starts with their attack at the α-C atom neighboring to one of the *N*-oxide groups followed by loss of the *N*-oxide oxygen atom and upon hydrolysis produces an α-OH substituent (*9*, *25*). Other studies generally believed that radicals of *N*-oxides are involved in the oxidation of QDX by photolytic, enzymatic, or electrochemical means (*26*−*29*). Radical intermediates are also involved in many manganese oxide-mediated oxidation systems (e.g., refs *13* and *14*). For example, phenoxy radicals of triclosan were found to be critical intermediates in its oxidation by manganese oxides to form oxidation products through coupling, further oxidation, and breakdown of the radicals.

It has been reported that substantial oxygen exchange occurs between hydroxyl groups in water and the oxygen anions on the α-$Fe_2O_3$ surfaces, which likely involves the interchange of terminal and bridging OH groups on the surfaces with hydroxyl groups in water (*30*). A similar exchange is expected in the $MnO_2$/water mixtures. In oxidation experiments conducted in $H_2{}^{18}O$, one would expect manganese oxide surfaces to be covered by $-{}^{18}OH$ groups via the previous oxygen exchange processes. Since oxidation of *N*-oxides by $MnO_2$ involves surface reaction, the observed $^{18}O$ atoms in the oxidation products of QNO are most likely derived from the surface bound $-{}^{18}OH$ groups.

On the basis of the experimental results and relevant studies listed previously, the oxidation pathway of QNO by manganese oxide is proposed in Scheme 1. In analogy to triclosan and other substituted phenols, QNO could be viewed as a phenoxy anion that, after forming a precursor complex with the oxide surface, would lose an electron to manganese oxide generating an *N*-oxide radical. *N*-Oxide radicals are most likely centered at the α-C rather than at the O atom due to the stronger electronegativity of O than C. Similar to phenoxy radicals, *N*-oxide radicals could undergo further oxidation leading to the generation of 2-hydroxyquinoline and *m*/*z* 305 products (an overall 2-electron transfer). The *m*/*z* 305 product may degrade further to eventually yield 2-hydroxyquinoline. Radical coupling to yield dimeric products was observed to be the dominant pathway in the oxidation of triclosan by manganese oxides (*14*). However, no appreciable amount of dimeric products could be detected in the current study. There are two possible reasons for this result. First, QNO and hence the corresponding QNO radicals do not adsorb significantly to the oxide surfaces. The low radical density at the surfaces would make it unlikely for radicals to couple with each other. Once radicals are released into the bulk solution, they are highly unstable under the mildly acidic conditions (*31*) and thus cannot survive long enough to undergo any coupling reactions. Second, the positive charge on the N atom of QNO radicals may lead to the formed dimeric products very unstable due to accumulation of positive charges.

Only a small amount of QXO was synthesized and purified for the kinetic study; thus, it was not examined for products. However, the oxidation mechanism of QXO is expected to resemble that of QNO. Other heterocyclic *N*-oxides will likely follow the previous reaction scheme as well in oxidation by manganese oxide. If two *N*-oxide groups are both reactive as in the case of QDX, other reaction pathways may also play a role, potentially due to interactions between the two *N*-oxide groups through resonance within the heterocyclic ring (*2*).

As discussed in an earlier section, substitution of *N*-oxide's α-H with alkyl groups significantly reduces the reactivity as in the cases of CDX and ODX. Such a substitution may create steric hindrance that prevents further reaction at the α-C position. An alterative explanation is that the α-H is critical in the further oxidation of *N*-oxide radicals, in which it hops to the neighboring O• on $MnO_2$ to release the reduced $Mn^{III}$ as shown in Scheme 1, a mechanism similar to that proposed by Chauhan et al. (*32*) in biomimetic oxidation of 1-naphthol by an Fe(III)-porphyrin complex system. Our study also showed that oxidation of QNO yielded predominantly 2-hydroxyquinoline (>95%), rather than other hydroxyquinoline isomers with the −OH group at different resonance positions. This result suggests that QNO likely interacts with manganese oxide surfaces via its *N*-oxide group, rendering further oxidation and hydroxylation at the position ortho to the *N*-oxide group much more likely at the oxide surfaces.

The inertness of 2-hydroxyquinoline and quinoxaline 2,3-diol products toward oxidation by $MnO_2$ may seem contradictory to the knowledge of fast oxidation of some phenols and catechol by manganese oxides (*13*, *14*, *33*, *34*). The electron-withdrawing effect of the heterocyclic nitrogen atom in a pyridine ring is similar to that of a nitro group (*35*), and it is known that electron-withdrawing substituents retard the oxidation of phenols by manganese oxides (e.g., refs *13* and *14*). Thus, the heterocyclic N atoms in 2-hydroxyquinoline and quinoxaline 2,3-diol can reduce these compounds' reactivity toward manganese oxides. Another plausible reason is caused by tautomerization of 2-hydroxyquinoline and quinoxaline 2,3-diol structures as shown in eq 2:


enol form keto form (2)

Earlier studies have reported that the keto-form of 2-hydroxyquinoline is more favorable in polar solvents such as water, while the enol-form is more favorable in nonpolar solvents (*36*−*38*). The keto-form is understandably much less susceptible to oxidation than the enol-form, thus explaining the low reactivity of 2-hydroxyquinoline and quinoxaline 2,3-diol to $MnO_2$ in water.

On the basis of the experimental results and the discussion to this point, the reaction pathway of CDX by manganese oxide is proposed in Scheme 2. In light of the comparable reaction rates between CDX and QXO, and the very slow reaction of desoxy-CDX, the oxidation of CDX's *N*-oxide group should be much faster than any reactions on the side chain. Thus, the intermediate I is postulated in analogy to the oxidation of QNO and QDX. Any further reactions would proceed from I, with the most likely one being oxidation at the hydrazone moiety (−CH═N−NH−) on the side chain in its unprotonated form (*39*).

Hydrazines (−NH−NH−) and hydrazides (−CO−NH−NH−) have been oxidized to azo compounds (−N═N−) by several oxidizing agents, including $MnO_2$ (*22*, *23*, *40*), silver (I) oxide (*35*), cobalt salts (*41*), phenylseleninic acid (*42*), and enzymes (*43*). The formed azo compounds would lose $N_2$ to generate radicals. Ketone hydrazones (>C═N−$NH_2$) were also documented to undergo similar oxidation resulting in diazo (>C═$N^+$═$N^-$) intermediates (*40*, *44*). Particular to our interest is the study on the oxidation of phenylhydrazone ($(Ph)_2$C═N−NH−Ph) with active Mn dioxide in benzene solvent (*45*). In that study, a pseudo allylic radical (−C•−N═N−) was generated after losing one electron to manganese oxide. This radical then combined with an −OH group from the oxide skeleton, lost another electron from the O atom, and finally lost $N_2$ resulting in the generation of the corresponding ketone and biphenyl. In analogy to that, manganese oxide produces a pseudo-allylic radical II from the intermediate I, with the C-centered resonance structure as the dominant form due to the lower electronegativity of C than N. The radical II would then abstract a hydroxyl group from the oxide surface resulting in the observed $m/z$ 279 intermediate. The $m/z$ 279 intermediate undergoes further oxidation in the presence of manganese oxide to generate $N_2$ and other unknown products.

Unfortunately, the intermediate I could not be detected by the electrospray LC/MS analyses. In fact, the inability to detect this intermediate was unexpected based on the fact that the structurally similar parent CDX exhibited a strong response in electrospray LC/MS. A possible reason for the inability to detect the intermediate I may be low concentration. It is probable that the hydrazone side chain in CDX is more reactive than the side chain in desoxy-CDX owing to the strong electron-withdrawing effect of the two quinoxaline heterocyclic N atoms in desoxy-CDX (*34*). In CDX, the electron-withdrawing effect of the heterocyclic N atoms is considerably reduced by the electron-donating O atoms. Thus, the intermediate I, once generated from CDX, may quickly undergo further oxidation at the side chain and remain at trace levels throughout the reaction. Further investigation on the products of CDX with different analytical approaches is needed and may shed more light on the CDX oxidation mechanism.

**Environmental Significance.** To the authors' knowledge, this is the first study to report high reactivity of heterocyclic *N*-oxides toward oxidation by manganese oxides, highlighting a new reaction pathway for organic *N*-oxides in aqueous soil and sediment systems and in potential industrial and chemical applications. The mechanisms of this new reaction pathway elucidated in this study provide the basis for predicting the reactivity and transformation of other organic *N*-oxide compounds with minerals. Results of this study also warrant further investigation on the potential reactions of organic *N*-oxides with environmentally important minerals and metal species other than manganese oxides.

As far as the abiotic attenuation of organic *N*-oxides in the sediment−water interface is concerned, although the adsorption of these compounds is typically low toward pure Mn dioxide, their moderate sorption to soils and sediments with the aid of organic matter in the presence may enable their interactions and thus degradation by minerals in the soil−water environment. The rate law of eq 1 allows estimation of initial reaction rate under ideal conditions (i.e., with pure $\delta$-$MnO_2$ in clean water matrix) for CDX and likely other *N*-oxides as well because of the similar initial reaction rates observed for comparable *N*-oxides. Considering that the reaction rate of chemicals is generally slower with soil metal oxides than with pure oxides owing to differences in oxide properties and the presence of competing cosolutes in the former (e.g., refs *14* and *17*), the initial rate derived in this study may be viewed as the maximum reactivity of *N*-oxides with manganese oxide. Other degradation pathways with reaction rates faster than this prediction will likely dominate the degradation of *N*-oxides. Otherwise, manganese oxide-facilitated oxidation will play an important role in the overall fate and transformation of organic *N*-oxides in the environment.

## Acknowledgments

This material is based upon work supported by the National Science Foundation under Grant 0229172. The authors thank Andrew Tartaglia for laboratory assistance in this study. The time and comments provided by three anonymous reviewers are also thanked for improving this paper.

## Supporting Information Available

LC/MS spectra of organic *N*-oxides and corresponding products in Table S1. This material is available free of charge via the Internet at http://pubs.acs.org.

## Literature Cited

(1) Albini, A.; Pietra, S. *Heterocyclic N-oxides*; CRC Press: Boston, 1991.
(2) Katritzky, A., R.; Lagowski, J. M. *Chemistry of the Heterocyclic N-oxides*; Academic Press: New York, 1971; Vol. 19.
(3) Gorrod, J. W.; Beckett, A. H. *Drug Metabolism in Man*; Taylor & Francis LTD: London, 1978.
(4) FAO/WHO. Joint expert committee on food additives: evaluation of certain veterinary drug residues in food. *Tech. Ser.* **1990**, *No. 799*, 45.
(5) JECFA 36th meeting of the joint FAO/WHO expert committee on food additives. *WHO Food Additives Ser.* **1991**, *No. 27*, 141.
(6) Hutchinson, M. J.; Young, P. Y.; Hewitt, S. A.; Faulkner, D.; Kennedy, D. G. Development and validation of an important

method for confirmation of the carbadox metabolite, quinoxaline-2-carboxylic acid, in porcine liver using LC-electrospray MS-MS according to revised EU criteria for veterinary drug residue analysis. *Analyst* **2002**, *127*, 342−346.
(7) Commission Regulation No. 2788/98. *Off. J. Eur. Commun.* **1998**.
(8) MacIntosh, A. I.; Neville, G. A. Liquid chromatographic determination of carbadox, desoxycarbadox, and nitrofurazones in pork tissues. *J.—Assoc. Off. Anal. Chem.* **1984**, *67*, 958−962.
(9) Kurasawa, Y.; Takada, A.; Kim, H. S. Progress in the chemistry of quinoxaline *N*-oxides and *N*,*N*′-dioxides. *J. Heterocyclic Chem.* **1995**, *32*, 1085−1114.
(10) Rabolle, M.; Spliid, N. H. Sorption and mobility of metronidazole, olaquindox, oxytetracycline, and tylosin in soil. *Chemosphere* **2000**, *40*, 715−722.
(11) Ingerslev, F.; Torang, L.; Loke, M.-L.; Halling-Sorensen, B.; Nyholm, N. Primary biodegradation of veterinary antibiotics in aerobic and anaerobic surface water simulation systems. *Chemosphere* **2001**, *44*, 865−872.
(12) Kolpin, D. W.; Furlong, E. T.; Meyer, M.; Thurman, E. M.; Zaugg, S. D.; Barber, L. B.; Buxton, H. T. Pharmaceuticals, hormones, and other organic wastewater contaminants in U. S. streams, 1999−2000: A national reconnaissance. *Environ. Sci. Technol.* **2002**, *36*, 1202−1211.
(13) Stone, A. T. Reductive dissolution of manganese(III/IV) oxides by substituted phenols. *Environ. Sci. Technol.* **1987**, *21*, 979−988.
(14) Zhang, H.; Huang, C. H. Oxidative transformation of triclosan and chlorophene by manganese oxides. *Environ. Sci. Technol.* **2003**, *37*, 2421−2430.
(15) Laha, S.; Luthy, R. G. Oxidation of aniline and other primary aromatic amines by manganese dioxide. *Environ. Sci. Technol.* **1990**, *24*, 363−373.
(16) Pizzigallo, M. D. R.; Ruggiero, P.; Crecchio, C.; Mascolo, G. Oxidation of chloroanilines at metal oxide surfaces. *J. Agric. Food Chem.* **1998**, *46*, 2049−2054.
(17) Li, H.; Lee, L. S.; Schulze, D. G.; Guest, C. A. Role of soil manganese in the oxidation of aromatic amines. *Environ. Sci. Technol.* **2003**, *37*, 2686−2693.
(18) Murray, J. W. Surface chemistry of hydrous manganese dioxide. *J. Colloid Interface Sci.* **1974**, *46*, 357−371.
(19) Coperet, C.; Adolfsson, H.; Khuong, T.-A. V.; Yudin, A. K.; Sharpless, K. B. A simple and efficient method for the preparation of pyridine *N*-oxides. *J. Org. Chem.* **1998**, *63*, 1740−1741.
(20) Massy, D. J. R.; McKillop, A. Selective monodeoxygenation of methyl 3-(2-quinoxalinylmethylene)carbazate $N^1$,$N^4$-dioxide (carbadox). *Synthesis* **1996**, 1477−1480.
(21) Miao, X.-S.; March, R. E.; Metcalfe, C. D. A tandem mass spectrometric study of the *N*-oxides, quinoline *N*-oxide, carbadox, and olaquindox, carried out at high mass accuracy using electrospray ionization. *Int. J. Mass Spectrom.* **2003**, *230*, 123−133.
(22) Haksar, C. N.; Malhotra, R. C.; Ramachandran, P. K. Oxidation of hydrazides of salicylic and substituted salicylic acids with active manganese dioxide. *Ind. J. Chem., Sect. B* **1979**, *17B*, 191−193.
(23) Bhatnagar, I.; George, M. V. Oxidation with metal oxides. III. Oxidation of diamines and hydrazines with manganese dioxide. *J. Org. Chem.* **1968**, *33*, 2407−2411.
(24) Zhang, H. Metal oxide-facilitated oxidation of antibacterial agents. Ph.D. thesis. Georgia Institute of Technology, School of Civil and Environmental Engineering, Atlanta, GA, 2004.
(25) Ahmed, Y.; Qureshi, M. I.; Habib, M. S.; Farooqi, M. A. Quinoxaline derivatives. XII. The reactions of quinoxaline 1,4-dioxides with acetic anhydride. *Bull. Chem. Soc. Jpn.* **1987**, *60*, 1145−1148.
(26) Shukun, L.; Hanqing, W. Radical mechanism in the photoreaction of organic *N*-oxides: some paradiazine *N*,*N*-dioxides. *Heterocycles* **1986**, *24*, 659−664.
(27) Inbaraj, J. J.; Motten, A. G.; Chignell, C. F. Photochemical and photobiological studies of tirapazamine (SR 4233) and related quinoxaline 1,4-di-*N*-oxide analogues. *Chem. Res. Toxicol.* **2003**, *16*, 164−170.
(28) Ganley, B.; Chowdhury, G.; Bhansali, J.; Daniels, J. S.; Gates, K. S. Redox-activated, hypoxia-selective DNA cleavage by quinoxaline 1,4-di-*N*-oxide. *Bioorg. Med. Chem.* **2001**, *9*, 2395−2401.
(29) Geletii, Y. V.; Strelets, V. V.; Shafirovich, V. Y.; Shilov, A. E. Cation radicals of heterocyclic *N*-oxides and their reactions. *Heterocycles* **1989**, *28*, 677−685.
(30) Henderson, M. A.; Joyce, S. A.; Rustad, J. R. Interaction of water with the (1 × 1) and (2 × 1) surfaces of α-$Fe_2O_3$(012). *Surf. Sci.* **1998**, *417*, 66−81.
(31) Kung, K. H.; McBride, M. B. Electron-transfer processes between hydroquinone and iron oxides. *Clays Clay Miner.* **1988**, *36*, 303−309.
(32) Chauhan, S. M. S.; Kalra, B.; Mohapatra, P. P. Oxidation of 1-naphthol and related phenols with hydrogen peroxide and potassium superoxide catalysed by 5,10,15,20-tetraarylporphyrinatoiron(III)chlorides in different reaction conditions. *J. Mol. Catal. A* **1999**, *137*, 85−92.
(33) Liu, C.; Huang, P. M. The influence of catechol humification on surface properties of metal oxides. *Spec. Publ.—R. Soc. Chem.* **2001**, *273 (Humic Substances)*, 253−270.
(34) McBride, M. B. Adsorption and oxidation of phenolic compounds by iron and manganese oxides. *Soil Sci. Soc. Am. J.* **1987**, *51*, 1466−1472.
(35) Iqbal, R.; Ebrahim, S.; Ziaulhaq, M. Some oxidation reactions of isomeric pyridinecarboxylic acid hydrazides. *Turkish J. Chem.* **1997**, *21*, 200−208.
(36) Vasudevan, D.; Dorley, P. J.; Zhuang, X. Adsorption of hydroxy pyridines and quinolines at the metal oxide−water interface: Role of tautomeric equilibrium. *Environ. Sci. Technol.* **2001**, *35*, 2006−2013.
(37) Katritzky, A. R. *Advances in Heterocyclic Chemistry*; Academic Press: New York, 1963.
(38) Elguero, J.; Marzin, C.; Katritzky, A. R.; Linda, P. *Advances in Heterocyclic Chemistry. Supplement 1: The Tautomerism of Heterocycles*; Academic Press: New York, 1976.
(39) Hongekar, M. L.; Patil, J. B. Kinetics and mechanism of oxidation of *n*-butyric and iso-butyric acid hydrazides by hexacyanoferrate(III) in acidic medium. *Ind. J. Chem., Sect. A* **1998**, *37A*, 493−497.
(40) Smith, M. B.; March, J. *March's Advanced Organic Chemistry*, 5th ed.; John Wiley & Sons: New York, 2001.
(41) Jacobs, R. L. Oxidation of *p*-toluenesulfonylhydrazide to 1,2-di(*p*-toluenesulfonyl)hydrazine. *J. Org. Chem.* **1977**, *42*, 571−573.
(42) Bath, S.; Laso, N. M.; Lopez-Ruiz, H.; Quiclet-Sire, B.; Zard, S. Z. A practical access to acyl radicals from acyl hydrazides. *Chem. Commun.* **2003**, *2*, 204−205.
(43) Johnsson, K.; Schultz, P. G. Mechanistic studies of the oxidation of isoniazid by the catalase peroxidase from mycobacterium tuberculosis. *J. Am. Chem. Soc.* **1994**, *116*, 7425−7426.
(44) Nishinaga, A.; Yamazaki, S.; Matsuura, T. Novel oxidative cleavage of a carbon−carbon bond in hydrazones by oxygenation with cobalt Schiff base complex. *Tetrahedron Lett.* **1986**, *27*, 2649−2652.
(45) Bhatnagar, I.; George, M. V. Oxidation of phenylhydrazones with manganese dioxide. *J. Org. Chem.* **1967**, *32*, 2252−2256.

*Received for review August 10, 2004. Revised manuscript received October 26, 2004. Accepted November 1, 2004.*

ES048753Z